INFLUENCE OF CHLORIDE AND HYDROXIDE IONS CONCENTRATIONS ON THE CORROSION BEHAVIOR OF AL AND AL-SI ALLOY

A. S. IBRAHIM*, W. A. GHANEM**, W. A. HUSSIEN*, N. K. SHEHATA* AND R. M. ABOU SHAHBA*

** Chemistry Department, Faculty of Science (Girls), Al-Azhar University, Nasr City, Cairo, Egypt*

*** Central Metallurgical Research and Development Institute (CMRDI).Tepen, Cairo, Egypt*

Abstract

The electrochemical behavior of Al and Al-Si alloy in NaCl and NaOH solutions have been studied in the absence and presence of some amino acids as corrosion inhibitor. Open-circuit measurements showed that both immersion potential ($E_{im.}$) and steady state potential ($E_{s.s.}$) decreased and become more negative as the concentration of NaCl and NaOH increased, while the rate of film thickening independed on the solutions concentrations. Cyclic anodic polarization curves indicated a small hysteresis loop raising the possibility of pitting as well as crevices corrosion. The studies revealed that both glycine and valine adsorbed on the electrode surface and inhibited both anodic and cathodic reactions. Due to the electron donating effect of methyl group in valine, valine was more effective in inhibition than glycine.

Keywords: aluminum; aluminum alloys; Corrosion; inhibition; polarization.

1. Introduction:

The service life of most engineering materials depends on their ability to resist degradation. Some metals are more intrinsically resistance to corrosion than others, either due to the fundamental nature of the electrochemical processes involved or due to the details of how reaction products form[1,2].

Due to many applications of aluminum and aluminum alloys, considerable attention has been devoted to the corrosion behavior of these materials in various aggressive aqueous environments covering the entire pH range. Aluminum is usually protected by a thin oxide film which has been formed either spontaneously (native films) or deliberately (e.g. anodic films). The solubility of the oxide film is negligible in neutral solutions (pH interval 4.0 to 8.5) at room temperature provided the solution does not contain activating anions, whereas heavy corrosion is observed both in acidic and alkaline media[1-3].

The goal of this study is to gain better insight the electrochemical behavior of Al and Al-Si alloy in sodium chloride and sodium hydroxide solutions and evaluate some amino acids as corrosion inhibitors in such media.

2. Experimental:

- **Materials:**

Two samples of aluminum electrodes of special grades have been tested. Typical values of their chemical compositions are given in Table (1).

Table (1): The chemical composition of aluminum electrodes (by wt. %)

Samples	Al	Si	Fe	Cu	Mn	Mg	Zn	Cr	Ni	Ti	Pb	V
Electrode (I)	99.8	0.040	0.038	0.015	0.0051	0.0074	0.0114	0.001	0.003	0.01	0.005	0.0057
Electrode (II)	95.8	**3.58**	**0.335**	0.014	0.013	0.005	0.025	0.012	0.008	**0.106**	0.010	0.008

Cylindrical electrodes with a working surface area of $1cm^2$ were used. Electrodes were enclosed in a glass tube fixing with araldite adhesive. The electrical contact was made through a thick copper wire soldered to inner side of electrode. Prior to each experiment, the surface of the working electrode was prepared by polishing with a sequence of emery paper (600, 800, 1000 and 1200), cleaning several times with deionized water and drying with acetone before immersing in test solution.

Adopted Techniques:

I. Open–Circuit Technique:

Open-circuit measurements were measured in different concentrations of NaCl and NaOH (1×10^{-3} to 1.0M) solutions. All measurements were carried out in convinantional glass cell at room temperature. The potential was recorded as a function of time till steady state values were observed by using electronic multimeter. The potentials were recorded with respect to a saturated calomel electrode (SCE).

II. Potentiodynamic Cyclic Anodic Polarization Technique:

Potentiodynamic cyclic anodic polarization (P.C.A.P) was measured using Volta Lab 40 (PGZ301) – Radiometer analytical. After attaining a steady rest potential ($E_{corr.}$), the electrode scanned at a rate of 10 mV/s.. A single compartment–cylindrical three electrodes glass cell of 250 ml capacity was used. All potentials were measured with respect to saturated calomel electrode (SCE) and platinum sheet used as auxiliary electrode. All measurements were performed in freshly prepared aerated solutions at room temperature ($25 \pm 2^{\circ}C$).

3. Result and Discussion:

I. Open–Circuit measurements:

The behavior of two aluminum electrodes in different concentrations of sodium chloride and sodium hydroxide ion solutions (1×10^{-3} to 1.0M) was studied.

As it is clear from Figs.(1, 2), in all NaCl concentrations for electrodes (I and II), the potential moves rapidly towards more negative (cathodic) values due to the dissolution of pre-immersion oxide layer. Then potential shifts in the anodic direction during the first 5 minutes of immersion. This evaluation is attributed to the adsorption of the chloride ions[3]. For increasing immersion times, the corrosion potential goes towards more positive values and keeps a constant value after a period of experiments due to the formation of a porous layer of alumina.

The same behavior was observed in all NaOH concentrations for the two aluminum electrodes, Figs.(3, 4) the initial sharp decrease in the open–circuit potential value is usually due to the dissolution of the surface oxide, which achieved when the minimum potential is reached. The slow increase observed in the curves after the potential minimum can be ascribed either to the growth of a surface oxide film or to the formation of surface hydride and anodic polarization of the surface by accumulation of impurities[4-6].

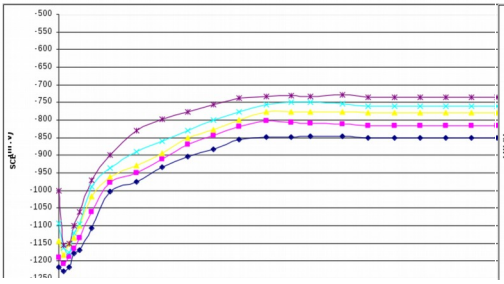

Fig. (1) : Potential / Time curves of electrode I in different NaCl concentrations

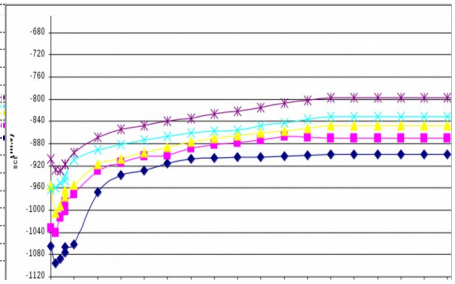

Fig. (2) : Potential / Time curves of electrode II in different NaCl concentrations

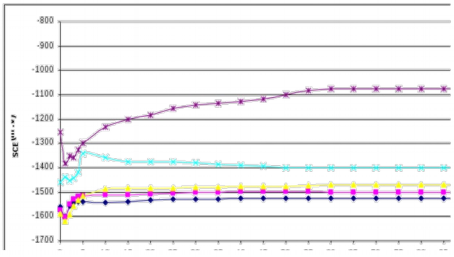

Fig. (3) : Potential / Time curves of electrode I in different NaOH concentrations

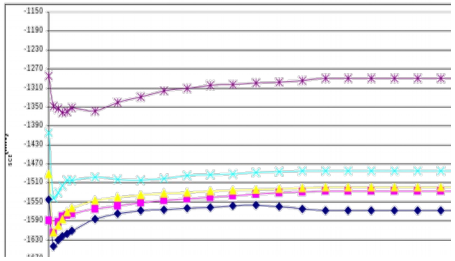

Fig. (4) : Potential / Time curves of electrode II in different NaOH concentrations

The immersion potentials ($E_{im.}$) as well as the steady state potential ($E_{s.s.}$) monitored for two aluminum electrodes, in various concentrations of NaCl and NaOH, decreased and become more negative as the concentration increases(Table 2).

Bracher[7] found that the steady – state potential, $E_{S.S}$, of a number of metal electrodes measured in aerated solutions of a number of anions changes with the anions concentration according to :

$$E_{S.S.} = a - b \log C \qquad (2)$$

where a and b are constants depending on the type of test solutions.

Depending on the variation of the steady – state potential of metal electrodes with logarithmic molar concentration, Figs.(5, 6), (a) can be calculated from the lines making the best fit with experimental results in solution of 1.0M concentration[7]. The values of (a) are: NaCl (-0.850 and -0.900V) and NaOH (-1.525 and -1.569V) for aluminum electrodes (I and II), respectively.

The results obtained from Fig.(5, 6) show that, the immersion potential and steady- state potential depend on the nature and composition of the aluminum electrodes. Also, comparing the activity of the two electrodes indicate that, the order runs as,

$$II > I$$

Table (2) Values of E_{imm} and $E_{S.S}$ for aluminum electrodes types (I and II)

	Electrodes	(I)		(II)	
	media	E_{imm} V	$E_{S.S}$ V	E_{imm} V	$E_{S.S}$ V
NaCl	1M	-1.217	-0.850	-1.065	-0.900
	0.5M	-1.190	-0.816	-1.033	-0.870
	0.1M	-1.144	-0.779	-0.956	-0.847
	0.01M	-1.093	-0.760	-0.963	-0.832
	0.001M	-1.001	-0.735	-0.907	-0.797
NaOH	1M	-1.559	-1.525	-1.546	-1.569
	0.5M	-1.575	-1.500	-1.590	-1.527
	0.1M	-1.590	-1.471	-1.491	-1.519
	0.01M	-1.459	-1.400	-1.404	-1.484
	0.001M	-1.253	-1.074	-1.284	-1.290

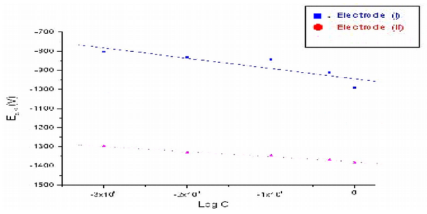

Fig. (5): $E_{S.S}$/log conc. Curves of electrode (I, II) in different concentrations of NaCl

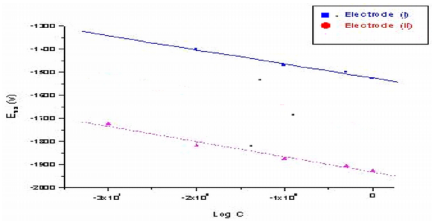

Fig.(6): $E_{S.S}$/log conc. Curves of electrode (I, II) in different concentrations of NaOH

II. Potentiodynamic cyclic anodic polarization measurements:

Figs.(7-10) represent the potentiodynamic cyclic anodic polarization (PCAP) measurements for aluminum electrodes I and II, in different concentrations of aerated NaCl and NaOH solution ranging from 1×10^{-5} M to 1×10^{-2} M, using scan rate 10 mV/sec in the potential range from -2.0 to 1.0 V_{SCE} at 25˚C.

Its obvious from Figs.(7, 8) of two aluminum electrodes in NaCl solutions, the polarization curves characterized by the appearance of active, passive and transpassive regions before oxygen evolution. After the corrosion potential, the anodic current density starts to increase to form the active region at low concentrations. The increase of the potential in the positive direction leads to increasing of the anodic current, which corresponds to the oxidation of aluminum to aluminum ions, with increasing the potential a passive film [$Al(OH)_3$, AlOOH and Al_2O_3] can form[8]. In the forward scan a passive current zone which was observed up to the onset of pitting, E_{pit}, followed by a marked increase in anodic current due to stable pit growth or pit propagation. Vigorous hydrogen evolution occurs at high currents. When the potential is lowered below E_{pit} (reverse scan), a hysteresis in the current indicates continued pit growth that stops when the potential is lowered than E_{prot}, identified by the potential at which the reverse curve intersects the forward one in the passive current region[9]. The small hysteresis loop indicates the possibility of pitting as well as crevice corrosion and suggesting the nucleation and growth of pitting corrosion at the point of potential break down ($E_{pit.}$). Although, the pitting corrosion was proceed by uniform thinning of the oxide film which cover whelms the pitting corrosion.

The same behavior was observed for electrodes I and II in NaOH solutions for all polarization curves, Figs.(9, 10), at different concentrations.

From the corrosion parameters, Tables (3, 4), it is observed that, the corrosion potential, E_{corr}, pitting potential, E_{pit}, protection potential, E_{port}, and pitting current, I_{pit}, decreased and become more negative as the concentration increases. However, corrosion current, I_{corr}, protection current, I_{prot}, and corrosion rate increased and become more positive as the concentration of chloride and hydroxide ions increased for the two aluminum electrodes.

Pitting was the major form of localized corrosion on the Al and Al-3%Si alloy and it is observed from the lower concentrations of NaCl up to the higher one. Pits were predominantly hemispherical and elliptical in shape. Pits or crevices are present in oxygenated chloride solution on the surface. The pits are hidden by the precipitation of a gelatinous film of $Al(OH)_3$ which surrounds the pit in the form of chimneys. The presence of $AlCl_3$ in the oxide film has been indicated by several studies[8]. The presence of this complex fosters the breakdown of the hydroxide films of boehmite and bayrite (α-AlOOH).

From the experimental results for electrodes I and II in NaOH solutions, it is indicated that the surface of aluminum is covered by oxide film. When immersed in alkaline solutions, the outer surface of film will dissolve; on the other hand, aluminum atom in the electrodes will diffuse toward surface, or oxygen toward electrode, and combine to form passive film. In some areas, the passive film is not very dense due to structure defects and is relatively more soluble, where its dissolution is faster than formation. In these areas the film is thinned down till causing pits, where aluminum electrode is exposed to solution and easier to undergo corrosion. Compared with the reduction of water, the reduction of oxygen can be neglected[10]. The corrosion process of aluminum electrodes in alkaline solution is usually considered as[11–14]:

1- The rate of cathodic reaction which occurs when aluminum corrodes in alkaline solution i.e.

$$e^- + H_2O \longrightarrow 1\backslash 2\ H_2 + OH^- \qquad (1)$$

is a function of the electrode potential not of pH.

2- Since the thickness of the anodic film on aluminum varies with pH, reaction rate is independent of the film thickness.

3- These observations are consistent with a mechanism where the electron reacts with water which is at the surface of the metal and incorporated in the anodic film.

4- The slow step in the anodic reaction i.e.

$$Al + 4\,OH^- \longrightarrow Al(OH)_4^- + 3e^- \qquad (2)$$

is the formation of aluminate from the anodic film on the electrode surface.

The formation of Fe-Si intermetallic at Al/Si interface causes depletion of Fe and Si and intergranular attack, which is observed in combination with pitting, this results confirmed with other authors[15].

From this point of view, the probability of stable pitting is dependent on the probability of activating sites capable of metastable pit growth and the probability of these metastable pits attaining stability[16]. Both these probabilities are higher in electrode II than electrode I in both of NaCl and NaOH solutions in a good agreement with the results obtained from the open circuit measurements.

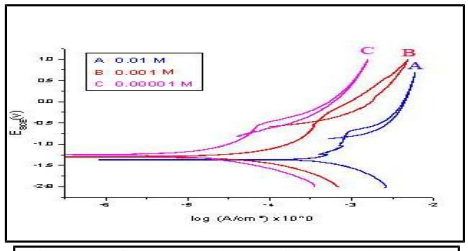

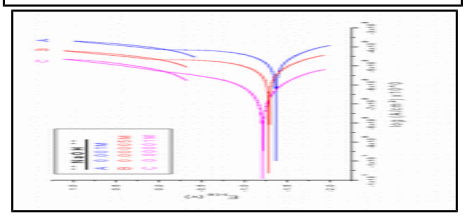

Fig. (9): Cyclic anodic polarization curves of eFig. (10): Cyclic anodic polarization curves of electrode (II) in different of NaOH solution concentrations of NaOH solution

Table (3): Electrochemical parameters of electrode (I and II) in NaCl solution:

	Conc. (M) ×10^{-2}	Corrosion rate mm/y	$I_{prot.}$ (A/cm^2)	I_{pit} (A/cm^2)	$I_{corr.}$ ×10^3 (A/cm^2)	$E_{prot.}$ (V)	E_{pit} (V)	$E_{corr.}$ (V)
Electrode (I)	**1**	-1.3595	-0.574630	-0.69657	0.077841	1.85×10^{-3}	1.19× 10^{-4}	0.108
	0.1	-1.3037	-0.24564	-0.46192	0.0092380	5.45× 10^{-4}	0.55× 10^{-4}	0.09004
	0.001	-1.1402	-0.18168	-0.72694	0.0067412	3.58×10^{-4}	1.05×10^{-5}	0.07884
	1	-1.2558	-0.33398	-0.6483	0.01607	2.18×10^{-4}	5.61×10^{-5}	0.1879
	0.1	-1.1907	0.01936	-0.2934	0.01008	4.24×10^{-5}	3.07×10^{-5}	0.1179

Electrode (II)	**0.001**	-0.6640	0.09146	-0.2852	0.001625	2.49×10^{-5}	2.76×10^{-6}	0.07313

Table (4): Electrochemical parameters of electrode (I and II) in NaOH solution:

	Conc. (M) $\times10^{-2}$	**Corrosion rate mm/y**	**$I_{prot.}$ (A/cm^2)**	**I_{pit} (A/cm^2)**	**$I_{corr.}\times10^3$ (A/cm^2)**	**$E_{prot.}$ (V)**	**E_{pit} (V)**	**$E_{corr.}$ (V)**
Electrode (I)	**1**	-1.4505	0.9123	__	0.0355	__	__	0.4147
	0.1	-1.3651	.0.9201	__	0.0126	__	__	0.1479
	0.001	-1.2921	0.9321	__	0.0114	__	__	0.1330
Electrode (II)	**1**	-1.4275	-0.2934	-1.4001	0.0244	3.07×10^{-7}	5.71×10^{-5}	0.2855
	0.1	-0.3454	0.4197	-0.0452	0.0095	3.11×10^{-5}	1.07×10^{-5}	0.1113
	0.001	-0.2444	0.6359	0.0946	0.0044	4.52×10^{-5}	6.21×10^{-6}	0.0518

In the present work, the effect of addition of different concentrations of glycine (NH_2CH_2COOH) and valine ($HO_2CCH(NH_2)CH(CH_3)_2$) as amino acids on the retardation of pitting corrosion of electrodes I and II in NaCl and NaOH solutions was studied.

As can be seen from Figs.(11-18), it is found that the values of corrosion potential, E_{corr}, pitting potential, E_{pit}, polarization resistance and inhibition efficiency increased and become more positive as the concentration of glycine and valine increased. However, the values of corrosion current, I_{corr} , pitting current I_{pit}, protection current, and protection potential, E_{prot}, decreased and become more negative with the increasing of the concentration of inhibitors.

From Figs.(11-18), it is found that at good conditions, the hysteresis loop observed during the reverse anodic scan which indicates the possibility of pitting corrosion is diminished as the concentration of glycine and valine added is increased. It is clear that the cathodic reaction (hydrogen evolution) is inhibited and inhibition increases as the inhibitor concentration increases.

In NaCl solutions, positive charge on nitrogen atom in glycine and valine might co-adsorbed on $AlCl_4^-$ type species, which were formed by the complexing of aluminum cation in oxide lattice with Cl^- anions, and prevent diffusion of $AlCl_4^-$ which is responsible for corrosion. So, the initial step of inhibition by amino acids is due to co-adsorption on $AlCl_4^-$ species[17]. At the isoelectric point, around pH = 6 in

this study, amino acids are in the form of zwitter ion[18]. Therefore, the results indicate chelation on metal surface occurs because zwitter ion forms of the studied amino acids are accepting electrons from metal which means they behaves as acceptors[17].

Glycine and valine affected both anodic and cathodic reactions, and the corrosion potential increased as the concentration increased so they are mixed inhibitors. Adsorption of these inhibitors on aluminum electrode surface obeys Langmuir and frumkin isotherms[19].

In NaOH solutions, small concentrations of the tested amino acids bring about marked decreased in corrosion current which depends on the nature of the substance added. As the concentration of the additive is raised, both glycine and valine yield decrease of corrosion current and represent monolayer coverage. This behavior can be explained by taking into consideration the fact that, in the basic solutions the adsorbability of the additives through either the dissociated carboxylate or the free amino group is considerably undermined. By analogy to the aliphatic acids, it is assumed that the amino acids are first adsorbed through their carboxylate end, leading to reduction in the dissolution rate. Thereafter, adsorption occurs mainly through the amino group of the molecule. Since the negatively charged $–COO^-$ rest is expected to weaken $–NH_2$ adsorption, relatively large concentration of additives is needed. Finally, glycine and valine in NaOH solutions act as anodic inhibitors[20].

In NaCl and NaOH solutions, for electrodes I and II, the comparison between the two inhibitors indicated that valine is more effective than glycine. This behavior is due to the electron donating effect of methyl group in valine which cause the electron density on the amino group will be higher than the electron density in amino group of glycine. Generally, the tested amino acids inhibition efficiencies increased as their concentration is increased and electrode I is more inhibited than electrode II in both glycine and valine.

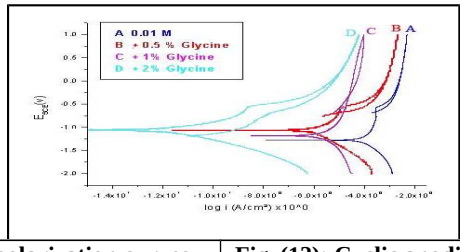

Fig. (11): Cyclic anodic polarization curves of electrode (I) in (0.01 M) sodium chloride solution with (0.5 – 2 %) glycine

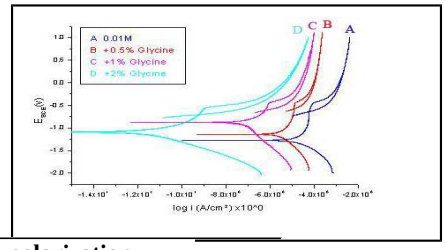

Fig. (12): Cyclic anodic polarization curves of electrode (II) in (0.01 M) sodium chloride solution with (0.5 – 2 %) glycine

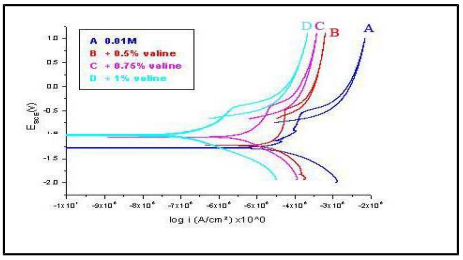

Fig. (13): Cyclic anodic polarization curves of electrode (I) in (0.01 M) sodium chloride solutionwith (0.5 – 1 %) valine

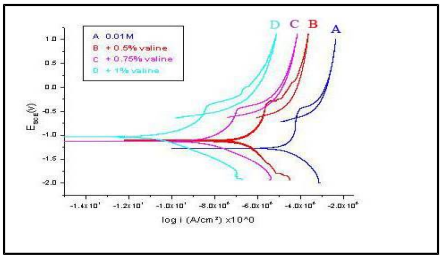

Fig. (14): Cyclic anodic polarization curves of electrode (II) in (0.01 M) sodium chloride solution with (0.5 – 1 %) valine

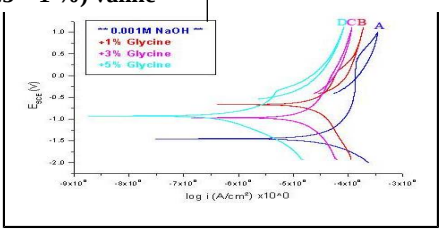

Fig. (15): Cyclic anodic polarization curves of electrode (I) in (0.001 M) sodium hydroxide solution with (1-5 %) glycine

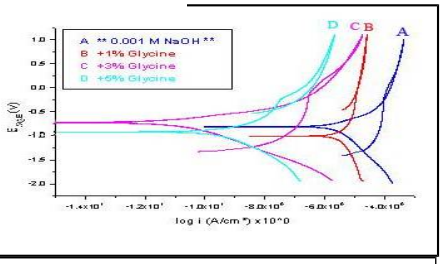

Fig. (16): Cyclic anodic polarization curves of electrode (II) in (0.001 M) sodium hydroxide solution with (1-5 %) glycine

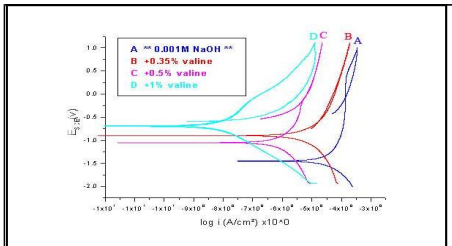

Fig. (17): Cyclic anodic polarization curves of electrode (I) in (0.001 M) sodium hydroxide solution with (0.35-1 %) valine

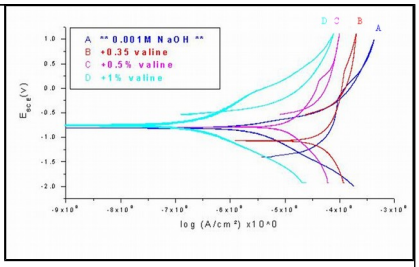

Fig. (18): Cyclic anodic polarization curves of electrode (II) in (0.001 M) sodium hydroxide solution with (0.35-1 %) valine

III- SEM:

It is clear from scanning electron microscopy (SEM) for aluminum electrode (II), the microstructure for specimens surface immersed in 0.01M NaCl, Fig.(19,a), and 0.001M NaOH, Fig.(20,a), showed heterogeneous surface morphology characterized by groves with some scattered pits. After addition of 2% glycine to 0.01M NaCl, Fig.(19,b), and 2%valine to 0.001M NaOH, Fig.(20,b), the attack was reduced and specimen kept their metallic luster with formation of adsorbed layer of the inhibitor on the electrode surface confirming the highest inhibition efficiency of glycine and valine.

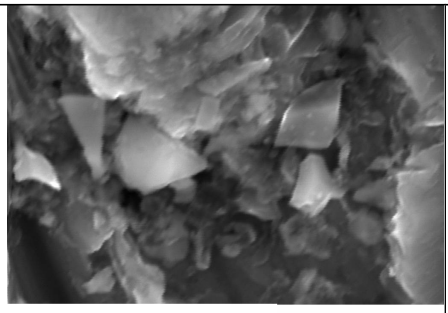

Fig.(19,a): Surface morphology for electrode II in 0. 01M NaCl

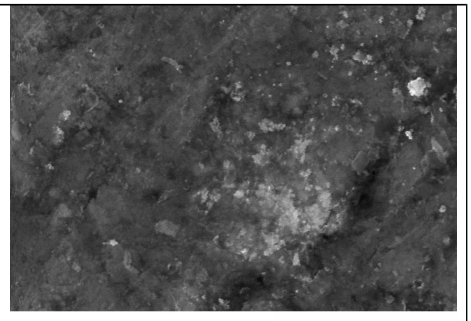

Fig.(19,b): Surface morphology for electrode II in0.01M NaCl with addition 2% glycine

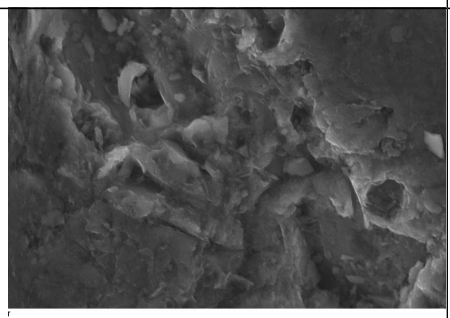

Fig.(20, a): Surface morphology for electrode II in 0. 001M NaOH

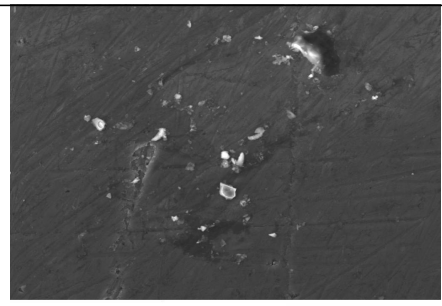

Fig.(20,b): Surface morphology for electrode II in 0.001M NaOH with addition 2% valine

4. Conclusion:

This study leads to the following:

a. Open-circuit measurements showed that both immersion potential ($E_{im.}$) and steady state potential ($E_{s.s.}$) for the two electrodes decreased and shifted to more negative values as the concentration of NaCl and NaOH increased.

b. Potentiodynamic cyclic anodic polarization curves indicated a small hysteresis loop denoting the possibility of pitting as well as crevices corrosion and suggesting the nucleation and pitting growth.
c. The formation of Fe-Si intermetallic at Al/Si interface caused depletion of Fe and Si and intergranular attack, which is observed in combination with pitting, these results explained the high activity of electrode II than electrode I in both NaCl and NaOH solutions in a good agreement with the results obtained from the open circuit measurements.
d. Glycine and valine represented monolayer coverage on the electrode surface and yielded decreasing in corrosion current by retardation both anodic and cathodic reactions.
e. Due to the electron donating effect of methyl group in valine, valine was more effective in inhibition than glycine for the two electrodes in both NaCl and NaOH solutions.

References:

1. D.Mercier and M.-G.Brthes-Labrouse, Corrosion Science, 51, p 339-348 (2009).

2. N. Hackerman, Corrosion-NACE, 18, p 332-337 (1962).

3. J. O,M. Bockris and L$_J$. V. Minevski, Journal of Electroanalytical chemistry, 349, p. 375 (1993).

4. - S. Adhikari and K. R. Hebert, Corrosion Science , 50, p.1414-1421 (2008).

5. S. M. Moon and S. I. Pyun, Journal of Solid State Electrochemistry, 3, p. 104-110 (1999).

6. S. I. Pyun, and S. M. Moon, Journal of Solid State Electrochemistry, 4, p. 267-272 (2000).

7. D. M. Brasher, Nature, London, 193, 868 (1962), " Proc, 2nd., European Symposium on Corrosion Inhibition.", Ferrara, Italy, 61 (1965).

8. J. H. de Boer, " Advances in Colloid Science ", vol.III, p.1, Inter Science Publishers, in H. Mark , E. J. W. Verwey (Eds) , New York (1950).

9. M. Yasuda, F. Weinberg and D. Tromans, Journal of Electrochemical Society, 137, p. 3708-3715 (1990).

10. D. D. Macdonald, S. Real, S. I. Smedley and M. Urquidi – Macdonald, Journal of Electrochemical Society, 135, p. 2410 (1988).

11. R. D. Armstrong and V. J. Braham, Corrosion Science, 38, p.1463(1996).

12. D. Chu and R. Savinell, Electrochemica Acta, 35, p.774 (1991).

13. A. A. Romanenkov and V.N. Gryslov, Russian Journal of Electrochemistry, 30, p.774 (1994).

14. M. L. Doche, J.J .Rameau, R. Durand and F. novel-Cattin, Corrosion Science, 41, p.805 (1999).

15. Z. Ahmed, P.T. Paulette and B.J.A. Aleem, Journal of Materials Science, 35, p.2573-2579 (2000).

16. E. McCafferty, Corrosion Science, 45, p.1421-1438 (2003).

17. A. Yurt, G. Bereket and C. Ogretir, Journal of Molecular Structure, Theo.chemistry, 725, p. 215-221 (2005).

18. B. Zaid, D. Saidi, A. Benzaid and S.Hadji, Corrosion Science, 50, n.7, p.1841-1847 (2008).

19. H. Ashassi - Sorkhabi, Z. Ghasemi and D. Seifzadeh, Applied Surface Science, 249, p.408-418 (2005).

20. R. M. Saleh and A. M. Shams Eldin, Corrosion Science, 12, p.689 (1972).